

Tumor-suppressive *microRNA-1291* directly regulates glucose transporter 1 in renal cell carcinoma

Takeshi Yamasaki,^{1,4} Naohiko Seki,^{2,4} Hirofumi Yoshino,¹ Toshihiko Itesako,¹ Yasutoshi Yamada,¹ Shuichi Tatarano,¹ Hideo Hidaka,¹ Tomokazu Yonezawa,¹ Masayuki Nakagawa¹ and Hideki Enokida^{1,3}

¹Department of Urology, Graduate School of Medical and Dental Sciences, Kagoshima University, Kagoshima; ²Department of Functional Genomics, Graduate School of Medicine, Chiba University, Chiba, Japan

(Received January 15, 2013/Revised July 9, 2013/Accepted July 21, 2013/Accepted manuscript online July 25, 2013/Article first published online August 22, 2013)

Our recent studies of microRNA (miRNA) expression signatures demonstrated that *microRNA-1291* (*miR-1291*) was significantly downregulated in renal cell carcinoma (RCC) clinical specimens and was a putative tumor-suppressive miRNA in RCC. The aim of the present study was to investigate the functional significance of *miR-1291* in cancer cells and to identify novel *miR-1291*-mediated cancer pathways and target genes in RCC. Expression of *miR-1291* was significantly downregulated in RCC tissues compared with adjacent non-cancerous tissues. Restoration of mature *miR-1291* in RCC cell lines (A498 and 786-O) revealed significant inhibition of cell proliferation, migration and invasion, suggesting that *miR-1291* functioned as a tumor suppressor. To identify *miR-1291*-mediated molecular pathways and targets, we used gene expression analysis (expression of RCC clinical specimens and *miR-1291*-transfected A498 cells) and *in silico* database analysis. Our data demonstrated that 79 signaling pathways were significantly regulated by tumor-suppressive *miR-1291* in RCC cells. Moreover, solute carrier family 2 member 1 (*SLC2A1*) was a candidate target of *miR-1291* regulation. The *SLC2A1* gene provides instructions for producing glucose transporter protein type 1 (*GLUT1*). Luciferase reporter assays showed that *miR-1291* directly regulated *SLC2A1/GLUT1*. In RCC clinical specimens, the expression of *SLC2A1/GLUT1* mRNA was significantly higher in cancer tissues than in non-cancerous tissues. A significant inverse correlation was recognized between *SLC2A1/GLUT1* and *miR-1291* expression ($r = -0.55$, $P < 0.0001$). Loss of tumor-suppressive *miR-1291* enhanced RCC cell proliferation, migration and invasion through targeting *SLC2A1/GLUT1*. The identification of novel tumor-suppressive *miR-1291*-mediated molecular pathways and targets has provided new insights into RCC oncogenesis and metastasis. (*Cancer Sci* 2013; 104: 1411–1419)

Renal cell carcinoma (RCC) is a disease in which cancer cells form in the tubules of the kidney. Globally, the incidence and mortality rates of RCC are increasing 2–3% per decade.⁽¹⁾ The 5-year survival rate of advanced-stage RCC is very poor (5–10%) due to recurrence or distant metastasis.⁽²⁾ The latest treatment for RCC includes molecular-targeted therapies, which have been developed and are widely used for patients with metastatic or recurrent RCC.⁽³⁾ However, these types of therapies are not expected to have curative effects.

The discovery of non-coding RNA (ncRNA) in the human genome was an important conceptual breakthrough in the post-genome sequencing era.⁽⁴⁾ Improved understanding of ncRNA is necessary for continued progress in cancer research. MicroRNA (miRNA) are endogenous small ncRNA molecules (19–22 bases in length) that regulate protein-coding gene expression by repressing translation or cleaving RNA transcripts in a sequence-specific manner.⁽⁵⁾ Currently, 2042 human mature miRNA are registered at miRBase release 19.0 (<http://microrna.sanger.ac.uk/>). MicroRNA are unique in their

ability to regulate multiple protein-coding genes. Bioinformatic predictions indicate that miRNA regulate more than 30% of the protein-coding genes in the human genome.⁽⁶⁾ A growing body of evidence suggests that miRNA are aberrantly expressed in many human cancers and that they play significant roles in the initiation, development and metastasis of these cancers.⁽⁷⁾ Some highly expressed miRNA can function as oncogenes by repressing tumor suppressors, whereas low-level miRNA can function as tumor suppressors by negatively regulating oncogenes.⁽⁸⁾ It is believed that normal regulatory mechanisms can be disrupted by aberrant expression of tumor-suppressive or oncogenic miRNA in cancer cells. Therefore, identification of aberrantly expressed miRNA is the first step toward elucidating miRNA-mediated oncogenic pathways.

Based on this idea, we identified miRNA expression signatures in RCC using clinical specimens. Our previous study indicated that *miR-1291* was significantly reduced in cancer tissues compared with adjacent non-cancerous tissues, suggesting that *miR-1291* is a candidate tumor-suppressive miRNA in human cancers.⁽⁹⁾ To the best of our knowledge, there are no publications about *miR-1291* in cancer biology. The aim of the present study was to investigate the functional significance of *miR-1291* and identify the molecular pathways and target genes regulated by *miR-1291* in RCC cells. Genome-wide gene expression analysis of *miR-1291* transfectants and *in silico* database analysis showed that solute carrier family 2 member 1 (*SLC2A1*) was a promising candidate target of *miR-1291*. The *SLC2A1* gene provides instructions for production of glucose transporter protein type 1 (*GLUT1*). *SLC2A1/GLUT1* facilitates the transport of glucose across the plasma membranes of mammalian cells. *SLC2A1/GLUT1* is responsible for the low level of basal glucose uptake required to sustain respiration in all cells. In malignant cells, the rate of glucose uptake is significantly accelerated and oxidative phosphorylation in mitochondria is often decreased compared with normal cells. This effect was first noted by Otto Warburg in 1929 and is called aerobic glycolysis or the Warburg effect.⁽¹⁰⁾ Transportation of glucose across the plasma membrane of cancer cells is the first rate-limiting step for glucose metabolism and increased glucose metabolism in cancer cells is associated with upregulation of the transport of glucose proteins. In fact, *SLC2A1/GLUT1* is overexpressed and is associated with poor prognosis in a wide range of cancers.^(11,12) Also, *SLC2A1/GLUT1* expression is affected by several signal pathways, such as cAMP, p53, insulin and oncogenic signaling.⁽¹³⁾ These data suggest that *SLC2A1/GLUT1* acts as an oncogene in human cancer cells. Thus, *SLC2A1/GLUT1* might be targeted by a putative tumor-suppressive *miR-1291* in RCC. Elucidation of tumor-suppressive miRNA-modulated cancer pathways will

³To whom correspondence should be addressed.
E-mail: enokida@m.kufm.kagoshima-u.ac.jp

⁴These authors contributed equally to this work.

provide new insights into the potential mechanisms of RCC oncogenesis and will facilitate the development of novel therapeutic strategies for the treatment of RCC.

Materials and Methods

Clinical specimens and cell culture. A total of 27 pairs of clear cell RCC (ccRCC) specimens and adjacent non-cancerous specimens were collected from patients who had undergone radical nephrectomies at Kagoshima University Hospital. The samples were processed and stored in RNAlater (QIAGEN, Valencia, CA, USA) at -20°C until RNA extraction. Patient information is summarized in Table 1. The samples were staged according to the American Joint Committee on Cancer–Union Internationale Contre le Cancer (UICC) tumor–node–metastasis classification and were histologically graded.⁽¹⁴⁾ The present study was approved by the Bioethics Committee of Kagoshima University; prior written informed consent and approval was given by each patient.

For cell culture experiments, we used two human RCC cell lines (A498 and 786-O) obtained from the American Type Culture Collection (Manassas, VA, USA). The cell lines were incubated in RPMI 1640 medium supplemented with 10% fetal bovine serum (FBS) and maintained in a humidified incubator (5% CO_2) at 37°C . Total RNA was extracted, as previously described.^(9,15) To evaluate epigenetic alterations of genomic methylation, these cells were treated with $1\ \mu\text{M}$ of the DNA methyltransferase inhibitor, 5-aza-dC (Sigma-Aldrich, St Louis, MO, USA). Cultured cells were harvested after 4 days of exposure to 5-aza-dC and the total RNA was extracted.

Quantitative real-time RT-PCR. TaqMan probes and primers for *SLC2A1/GLUT1* (P/N: Hs00892681_m1; Applied Biosystems, Foster City, CA, USA) were assay-on-demand gene expression products. All reactions were performed in duplicate and a negative control lacking cDNA was included. We followed the manufacturer's protocol for PCR conditions. Stem-loop RT-PCR (TaqMan MicroRNA Assays; P/N: 002838 for *miR-1291*; Applied Biosystems) was used to quantify miRNA according to earlier published conditions.⁽¹⁶⁾ To normalize the data for quantification of *GLUT1* mRNA and the miRNA, we used *human GUSB* (P/N: Hs99999908_m1; Applied Biosys-

tems) and *U6* (P/N: 001973; Applied Biosystems), respectively. The delta–delta Ct method was used to calculate the fold change.

Mature miRNA. As described previously,^(9,17) RCC cell lines were transfected with Lipofectamine RNAiMAX transfection reagent (Invitrogen, Carlsbad, CA, USA) and Opti-MEM (Invitrogen) with $10\ \text{nM}$ mature miRNA molecules (P/N: AM17100; Ambion, Austin, TX, USA; and P/N: C-301345-00-0005; Thermo Fisher Scientific, Waltham, MA, USA). Pre-miR miRNA precursor-negative control (P/N: AM17111; Applied Biosystems) was used in the gain-of-function experiments. Cells were seeded in 10-cm dishes for protein extraction (8×10^5 cells per dish), six-well plates for wound healing assays (20×10^4 cells per well), 24-well plates for mRNA extraction and Matrigel invasion assays (5×10^4 cells per well) and 96-well plates for XTT assays (3×10^3 cells per well).

Cell proliferation, migration, invasion assays and cell cycle assays. Cell proliferation was determined using a XTT assay (Roche Applied Science, Tokyo, Japan) performed according to the manufacturer's instructions. Cell migration activity was evaluated with a wound healing assay. Cells were plated in six-well dishes and the cell monolayer was scraped using a P-20 micropipette tip. The initial gap length (0 h) and the residual gap length at 24 h after wounding were calculated from photomicrographs. A cell invasion assay was carried out using modified Boyden chambers consisting of Transwell-precoated Matrigel membrane filter inserts with $8\ \mu\text{m}$ pores in 24-well tissue culture plates (BD Biosciences, Bedford, MA, USA). Minimum essential medium containing 10% FBS in the lower chamber served as the chemoattractant as described previously.⁽¹⁵⁾ A cell cycle assay was performed using flow cytometry. The 786-O and A498 cells were transiently transfected with miR-control or *miR-1291* and were harvested 72 h after transfection using trypsinisation. These cultured cells were incubated in $200\ \mu\text{L}$ of Krishan's reagent (0.05 mg/mL propidium iodide, 0.1% sodium citrate, 0.02 mg/mL RNase A, 0.3% Nonidet P-40, pH 8.3), then fluorescence from propidium iodide–nuclear DNA complexes was analyzed with a FACSCalibur (BD Bioscience). The percentage of cells in the G0/G1, S and G2/M phases were counted and compared. The apoptosis analysis was done as previously described.⁽¹⁷⁾ All experiments were performed in triplicate.

Screening of *miR-1291*-regulated genes using *in silico* and microarray data. To obtain putative *miR-1291* regulated genes, we used TargetScan database searching (<http://www.targetscan.org>). As another method, an oligo-microarray Human 44K (Agilent Technologies, Santa Clara, CA, USA) was used for expression profiling in *miR-1291*-transfected A498 cells and was compared with miR-transfected cells, as previously described.^(9,17) Briefly, hybridization and washing steps were performed in accordance with the manufacturer's instructions. The arrays were scanned using a Packard GSI Lumonics Scan-Array 4000 (PerkinElmer, Boston, MA, USA). The data obtained were analyzed with DNASIS array software (Hitachi Software Engineering, Tokyo, Japan), which converted the signal intensity into expression data. Data from each microarray study were subjected to global normalization.

Pathway analysis and expression data of putative *miR-1291* target genes. We performed gene expression analysis using *miR-1291* transfectants. To identify molecular targets and signaling pathways regulated by *miR-1291*, *in silico* and gene expression data were analyzed in Kyoto Encyclopedia of Genes and Genomics (KEGG) pathway categories using the GENECODIS program. In the present study, we focused on the 'pathways in cancer' category, which included 74 genes. Gene expression data was applied using the GEO database (GSE36895 and GSE22541).

Table 1. Patient characteristics

	n (%)
Total number	27
Median age (range) (years)	67 (42–86)
Gender	
Male	17 (63.0)
Female	10 (37.0)
Pathological tumor stage	
pT1	22 (81.5)
pT2	0 (0.0)
pT3	5 (18.5)
pT4	0 (0.0)
Grade	
G1	6 (22.2)
G2	20 (74.1)
G3	0 (0.0)
Unknown	1 (3.7)
Infiltration	
α	8 (29.6)
β	19 (70.4)
γ	0 (0.0)
Venous invasion	
No	20 (74.1)
Yes	7 (25.9)

Western blotting. After 3 days of transfection, protein lysates (50 μ g) were separated using NuPAGE on 4–12% bis-tris gels (Invitrogen) and transferred into polyvinylidene fluoride membranes. Immunoblotting was conducted with diluted (1:1000) polyclonal GLUT1 antibodies (catalog number, C0213; Assay Biotechnology, Sunnyvale, CA, USA) and GAPDH antibodies (catalog number, MAB374; Chemicon, Temecula, CA, USA). The membrane was washed and then incubated with goat anti-rabbit IgG (H+L)-HRP conjugate (Bio-Rad, Hercules, CA, USA). Specific complexes were visualized with an echochemiluminescence detection system (GE Healthcare, Little Chalfont, UK) and the expression levels of these genes were evaluated using ImageJ software (ver. 1.43; <http://rsbweb.nih.gov/ij/index.html>).

Plasmid construction and dual-luciferase reporter assay. MicroRNA target sequences were inserted between the *XhoI*-*PmeI* restriction sites in the 3'UTR of the *hRluc* gene in the psiCHECK-2 vector (C8021; Promega, Madison, WI, USA). 786-O cells were transfected with 15 ng vector, 10 nM microRNA and 1 μ L Lipofectamine 2000 (Invitrogen) in 100 μ L Opti-MEM (Invitrogen). The activities of firefly and *Renilla* luciferases in cell lysates were determined using a dual-luciferase assay system (E1910; Promega). Normalized data were calculated as the ratio of *Renilla*/firefly luciferase activities.

Statistical analysis. The relationships between two variables and numerical values were analyzed using the Mann–Whitney *U*-test and the relationship between three variables and numerical values was analyzed using the Bonferroni-adjusted Mann–Whitney *U*-test. The relationship between *miR-1291* expression and *GLUT1* mRNA expression was analyzed using the Spearman rank correlation. Expert Stat View analysis software (ver. 4; SAS Institute Inc., Cary, NC, USA) was used in these analyses. In the comparison of three variables, a non-adjusted statistical level of significance of $P < 0.05$ corresponded to the Bonferroni-adjusted level of $P < 0.0167$.

Results

Expression of *miR-1291* in RCC clinical specimens and cancer cell lines. We showed the gene structure of *miR-1291* in the 12q13.11 region of the human genome (Fig. 1a). The *miR-1291* is nested in an intron of the *KAT8* regulatory NSL complex subunit 2 (*KANSL2*) gene. First, we evaluated *miR-1291*

expression in RCC clinical specimens and RCC cell lines using real-time PCR analysis. The relative expression of *miR-1291* to an internal control (U6) was significantly lower in clinical RCC specimens ($n = 27$; 0.0001014 ± 0.000168) than in adjacent non-cancerous specimens ($n = 27$; 0.001 ± 0.002 , $P < 0.0001$; Fig. 1b). In contrast, there was no significant difference in *KANSL2* mRNA relative to *GUSB* between clinical RCC specimens ($n = 27$; 0.269 ± 0.232) and adjacent non-cancerous specimens ($n = 27$; 0.326 ± 0.315 , $P = 0.6938$; Fig. 1c). Also, we could not find any positive correlations between *KANSL2* mRNA and *miR-1291* expression. These data suggest that they might have different mechanisms to regulate their expression even though *miR-1291* is nested in the *KANSL2* gene.

We also evaluated the expression levels of *miR-1291* in RCC cell lines. *miR-1291* expression levels in A498 and 786-O cells were significantly lower than those in non-cancerous kidney tissues ($P < 0.0001$; Fig. 1b). Furthermore, we investigated the expression of other types of human cancer cell lines (20 cell lines) and the expression level of *miR-1291* was ubiquitously low in other cancer cell lines as well as the RCC cell lines (Fig. S1).

To investigate the silencing mechanisms of *miR-1291*, we evaluated the expression levels of *miR-1291* in the RCC cells treated with a demethylating agent, 5-aza-dC. However, we could not find any restoration of *miR-1291* expression after 5-aza-dC treatment (data not shown).

Effects of *miR-1291* restoration on cell proliferation, migration and invasion in RCC cell lines. To investigate the functional role of *miR-1291*, we performed gain-of-function studies using cells transfected with mature *miR-1291*. We used two sources of mature *miR-1291* (Ambion and Thermo) to ensure reproducibility. The XTT assay demonstrated that cell proliferation was significantly inhibited in *miR-1291* transfectants in comparison with mock- or miRNA-control-transfected cells. Specifically, we observed the following growth rates, expressed as a percentage of the control, using Ambion miRNA: (i) A498: mock, $100.0 \pm 1.7\%$; miR-control, $98.4 \pm 0.5\%$; and *miR-1291*, $56.5 \pm 3.1\%$; and (ii) 786-O: mock, $100.0 \pm 1.2\%$; miR-control, $89.9 \pm 0.7\%$; and *miR-1291*, $59.1 \pm 0.6\%$, with $P < 0.0001$ for *miR-1291* in both cells lines (Fig. 2a). In contrast, Thermo miRNA gave the following growth rates: (i) A498: mock, $100.0 \pm 2.6\%$; miR-control, $94.6 \pm 1.7\%$; and

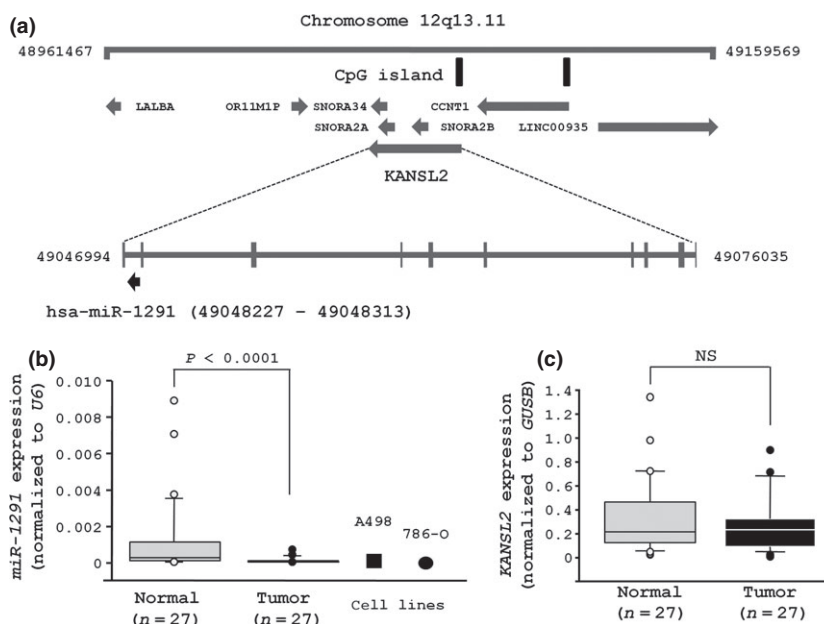


Fig. 1. Expression levels of *miR-1291* in renal cell carcinoma (RCC) clinical specimens, non-cancerous kidney tissues and RCC cell lines. Expression of *miR-1291* was significantly lower in 27 clinical RCC specimens and in RCC cell lines than in 27 adjacent non-cancerous specimens.

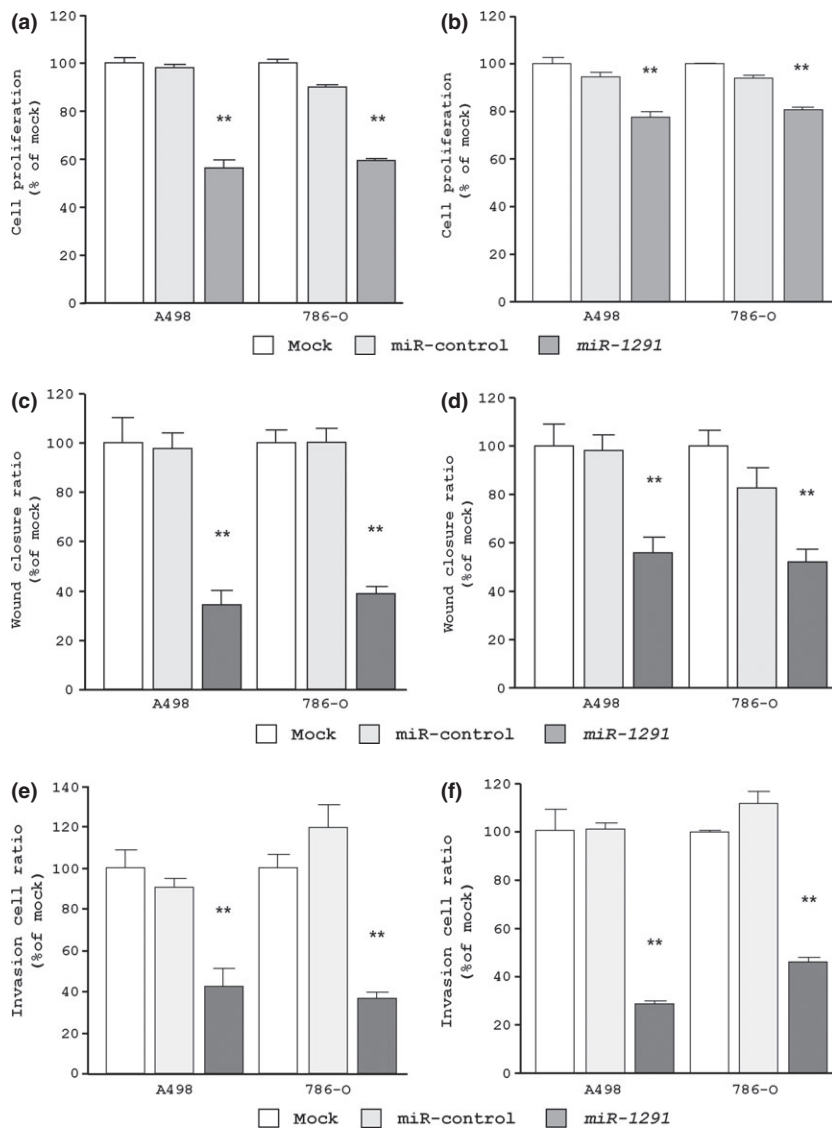


Fig. 2. Effects of *miR-1291* transfection on cell viabilities in renal cell carcinoma cell lines (A498 and 786-O). We used two sources of mature *miR-1291* from Ambion (a,c,e) and Thermo (b,d,f) to ensure reproducibility. (a,b) Cell proliferation determined using the XTT assay. (c,d) Cell migration activity determined using the wound healing assay. (e,f) Cell invasion activity determined using the Matrigel invasion assay. ** $P < 0.0001$.

miR-1291, $77.6 \pm 2.3\%$; and (ii) 786-O: mock, $100.0 \pm 0.7\%$; miR-control, $94.0 \pm 0.9\%$; *miR-1291*, $80.4 \pm 1.4\%$, with $P < 0.0001$ for *miR-1291* in both cell lines (Fig. 2b).

The wound healing assay demonstrated that significant inhibition of cell migration occurred in *miR-1291* transfectants in comparison with mock and miR-control transfectants. Specifically, we observed the following wound closure rates, expressed as a percentage of the control, using Ambion miRNA: (i) A498: mock, $100.0 \pm 10.2\%$; miR-control, $97.2 \pm 6.6\%$; and *miR-1291*, $34.3 \pm 5.7\%$; and (ii) 786-O: mock, $100.0 \pm 4.8\%$; miR-control, $99.8 \pm 5.7\%$; and *miR-1291*, $38.6 \pm 3.3\%$, with $P < 0.0001$ for *miR-1291* in both cell lines (Fig. 2c). In contrast, Thermo miRNA gave the following wound closure rates: (i) A498: mock, $100.0 \pm 9.0\%$; miR-control, $98.1 \pm 6.2\%$; and *miR-1291*, $55.8 \pm 5.9\%$; and (ii) 786-O: mock, $100.0 \pm 6.5\%$; miR-control, $82.8 \pm 0.8\%$; and *miR-1291*, $51.7 \pm 5.1\%$, with $P < 0.0001$ for *miR-1291* in both cell lines (Fig. 2d).

The Matrigel invasion assay demonstrated that the number of invading cells was significantly decreased in *miR-1291*-transfectants in comparison with mock and miR-control transfectants. Specifically, we observed the following invasion rates, expressed as a percentage of the control, using Ambion miRNA: (i) A498: mock, $100.0 \pm 8.9\%$; miR-control,

$90.7 \pm 4.1\%$; and *miR-1291*, $42.0 \pm 9.4\%$; and (ii) 786-O: mock, $100.0 \pm 6.3\%$; miR-control, $119.4 \pm 10.7\%$; and *miR-1291*, $36.2 \pm 3.3\%$, with $P < 0.0001$ for *miR-1291* in both cell lines (Fig. 2e). In contrast, Thermo miRNA gave the following invasion rates: (i) A498: mock, $100.0 \pm 14.7\%$; miR-control, $101.3 \pm 2.1\%$; and *miR-1291*, $28.7 \pm 1.4\%$; and (ii) 786-O: mock, $100.0 \pm 0.9\%$; miR-control, $112.0 \pm 4.9\%$; and *miR-1291*, $46.1 \pm 2.1\%$, with $P < 0.0001$ for *miR-1291* in both cell lines (Fig. 2f).

To investigate the anti-proliferative role of *miR-1291*, we performed cell cycle and apoptosis assays using flow cytometry. We found a marked G0-G1 arrest in *miR-1291*-transfected A-498 cells but not in 786-O cells (Fig. S2). We did not find any apoptotic effect in the *miR-1291*-transfected RCC cell lines (data not shown).

Identification of *miR-1291*-mediated molecular pathways and putative target genes in RCC. To gain further insight into the molecular mechanisms and pathways regulated by tumor-suppressive *miR-1291* in RCC, we first obtained putative *miR-1291* target genes by searching the TargetScan database. According to the database, 3363 conserved targets, with a total of 334 conserved sites and 4318 poorly conserved sites were deposited in this database. These genes were analyzed and characterized in KEGG pathway categories using the

GENECODIS 3.0 program. Our strategy for selection of *miR-1291* target genes is shown in Figure S3. This analysis revealed 79 signaling pathways that were significantly associated with the *miR-1291* target genes (Table S1) and the top 30 significant signaling pathways are listed in Table 2. In these pathways, we focused on the ‘pathways in cancer’ category because it was most significantly associated with *miR-1291*-regulated pathways in this analysis; 74 genes were contained within this pathway (Table S2).

To search for target genes in RCC regulated by tumor-suppressive *miR-1291*, we used two types of gene expression profiles. One was gene expression data of RCC clinical specimens and the other was analysis of gene expression in *miR-1291*-transfected A498 cells. First, we applied gene expression profiles in the GEO database (accession numbers GSE36895 and GSE22541) to evaluate upregulated or downregulated genes in RCC specimens. Among the 74 genes in the ‘pathways in cancer’ category, 12 were upregulated in 53 RCC clinical specimens compared with 23 non-cancerous kidney tissues (Table 3, Fig. 3). Precise information on all 74 genes is summarized in Table S3. Furthermore, to identify *miR-1291*-regulated genes, we performed genome-wide gene expression analysis using *miR-1291*-transfected A498 cells in comparison with miR-control transfectants. We searched for target genes regulated by tumor-suppressive *miR-1291* based on the following hypotheses: target genes should be upregulated in RCC specimens and downregulated in *miR-1291*-transfected cells. As a result of merging these two types of expression data, two

Table 2. Significantly enriched annotations regulated by *miR-1291* in the TargetScan database

No. genes	P-value	Annotations
74	5.69E-08	Pathways in cancer
61	6.63E-07	MAPK signaling pathway
40	2.64E-06	Wnt signaling pathway
44	2.82E-06	Calcium signaling pathway
35	5.66E-06	Axon guidance
47	6.09E-06	Endocytosis
39	8.83E-06	Jak-STAT signaling pathway
33	1.58E-05	Glutamatergic synapse
47	1.92E-05	Regulation of actin cytoskeleton
28	2.10E-05	GnRH signaling pathway
26	5.23E-05	Fc gamma R-mediated phagocytosis
27	5.31E-05	Melanogenesis
33	6.29E-05	Cell adhesion molecules
22	7.53E-05	Arrhythmogenic right ventricular cardiomyopathy
32	1.78E-04	Insulin signaling pathway
40	1.98E-04	Chemokine signaling pathway
30	2.02E-04	Neurotrophin signaling pathway
18	2.06E-04	Acute myeloid leukemia
24	2.13E-04	Dilated cardiomyopathy
51	2.27E-04	Cytokine–cytokine receptor interaction
20	2.54E-04	Adipocytokine signaling pathway
23	3.18E-04	ErbB signaling pathway
22	4.29E-04	Hypertrophic cardiomyopathy
18	5.46E-04	Colorectal cancer
16	6.16E-04	mTOR signaling pathway
18	6.35E-04	Glioma
20	7.29E-04	VEGF signaling pathway
19	7.80E-04	Pancreatic cancer
19	7.80E-04	Renal cell carcinoma
16	8.49E-04	Non-small-cell lung cancer

MAPK, mitogen-activated protein kinase; VEGF, vascular endothelial growth factor.

genes (*SLC2A1* and phosphoinositide-3-kinase, catalytic, gamma polypeptide [*PIK3CG*]) were listed as candidate *miR-1291* target genes in RCC (Table 3). Among these two potential targets, we focused on *SLC2A1/GLUT1* as a promising candidate target gene for *miR-1291* and considered whether *SLC2A1/GLUT1* was a direct target of *miR-1291*. We did not focus on the *PIK3CG* gene because there was no significant inverse correlation between *PIK3CG* and *miR-1291* expression, although the expression of *PIK3CG* was significantly higher in cancerous tissues (data not shown).

SLC2A1/GLUT1 is a direct target of *miR-1291* in RCC. Next, we performed quantitative real-time RT-PCR and western blotting to investigate whether *SLC2A1/GLUT1* mRNA and protein were downregulated by restoration of *miR-1291*. Importantly, both *SLC2A1/GLUT1* mRNA and protein levels were significantly repressed in *miR-1291*-transfectants in comparison with mock or miRNA-control transfectants (Fig. 4a,b).

To determine whether the 3'UTR of *SLC2A1/GLUT1* has an actual target site for *miR-1291*, we performed a luciferase reporter assay by using two partial vectors encoding the 3'UTR of *SLC2A1/GLUT1* mRNA including either binding site (position 607–613 or position 649–655). We found that the luminescence intensity was significantly reduced in the presence of either site targeted by *miR-1291* ($P < 0.05$; Fig. 4c). In contrast, luminescence intensity was not decreased when the seed sequence of both target sites was deleted from the vectors (Fig. 4c).

Expression of *SLC2A1/GLUT1* in RCC clinical specimens. Expression of *SLC2A1/GLUT1* mRNA was significantly higher in the 27 clinical RCC specimens than in the 27 adjacent normal specimens (clinical RCC specimens, 8.806 ± 1.192 ; adjacent normal tissues, 1.683 ± 0.378 ; $P < 0.0001$; Fig. 5a). The correlation between *SLC2A1* mRNA expression and *miR-1291* expression was investigated in clinical specimens. A significant inverse correlation was recognized between *SLC2A1/GLUT1* and *miR-1291* expression ($r = -0.55$, $P < 0.0001$; Fig. 5b).

Discussion

Aberrant expression of miRNA causes destruction of tightly regulated miRNA-protein-coding RNA networks in human cancer cells. Accumulating evidence of abnormally expressed miRNA in human cancers has demonstrated these miRNA-mediated functions and has shown that differentially expressed miRNA contribute to cancer initiation, development and metastasis.^(8,18) Based on these points, identification of aberrantly expressed miRNA-mediated cancer pathways and target genes is the first step in elucidating the role of miRNA in human cancers. To better understand RCC oncogenesis, we sequentially identified tumor-suppressive miRNA-mediated RCC molecular pathways based on RCC miRNA expression signatures.⁽⁹⁾ Recently, our miRNA studies in RCC revealed that *miR-1/133a*, *miR-138*, *miR-135a* and *miR-1285* function as tumor suppressors, inhibiting cell proliferation, migration and invasion through targeting *transgelin-2*, *vimentin*, *c-MYC* and *transglutaminase-2*, respectively.^(9,17,19,20)

Our previous study of RCC miRNA expression signatures showed that *miR-1291* was significantly downregulated, suggesting that this miRNA was a candidate tumor-suppressive miRNA in RCC. First, we evaluated the expression levels of *miR-1291* in RCC clinical specimens, and confirmed that *miR-1291* was significantly downregulated in tumor tissues. In addition, the expression level of *miR-1291* was ubiquitously low in 20 different cancer cell lines including RCC, glioblastoma, esophageal, breast, colon, bladder and prostate cancers. *MIR-1291* is uniquely nested in the *KANSL2* gene, which has CpG islands adjacent to its exon 1. However, the present study demonstrated that *miR-1291* expression did not depend on the methylation status of the host gene. Also, we could not

Table 3. Candidate target genes of *miR-1291* involved in 'pathways in cancer'

Expression (log2 ratio)		Entrez gene ID number	Symbol	Gene name
RCC clinical specimens	<i>miR-1291</i> transfectant			
2.47	-0.10	5880	RAC2	Ras-related C3 botulinum toxin substrate 2 (rho family, small GTP binding protein Rac2)
2.40	-0.42	2256	FGF11	Fibroblast growth factor 11
1.93	-1.04	6513	SLC2A1	Solute carrier family 2 (facilitated glucose transporter), member 1
1.77	-0.03	1029	CDKN2A	Cyclin-dependent kinase inhibitor 2A (melanoma, p16, inhibits CDK4)
1.47	0.01	1284	COL4A2	Collagen, type IV, alpha 2
1.39	1.69	23533	PIK3R5	Phosphoinositide-3-kinase, regulatory subunit 5
1.39	-0.21	5900	RALGDS	Ral guanine nucleotide dissociation stimulator
1.32	0.13	7039	TGFA	Transforming growth factor alpha
1.32	-0.68	2113	ETS1	V-ets erythroblastosis virus E26 oncogene homolog 1 (avian)
1.24	0.12	1438	CSF2RA	Colony stimulating factor 2 receptor alpha Low affinity (granulocyte-macrophage)
1.20	-0.01	5371	PML	Promyelocytic leukemia
1.20	-2.11	5294	PIK3CG	Phosphoinositide-3-kinase, catalytic, gamma polypeptide

RCC, renal cell carcinoma.

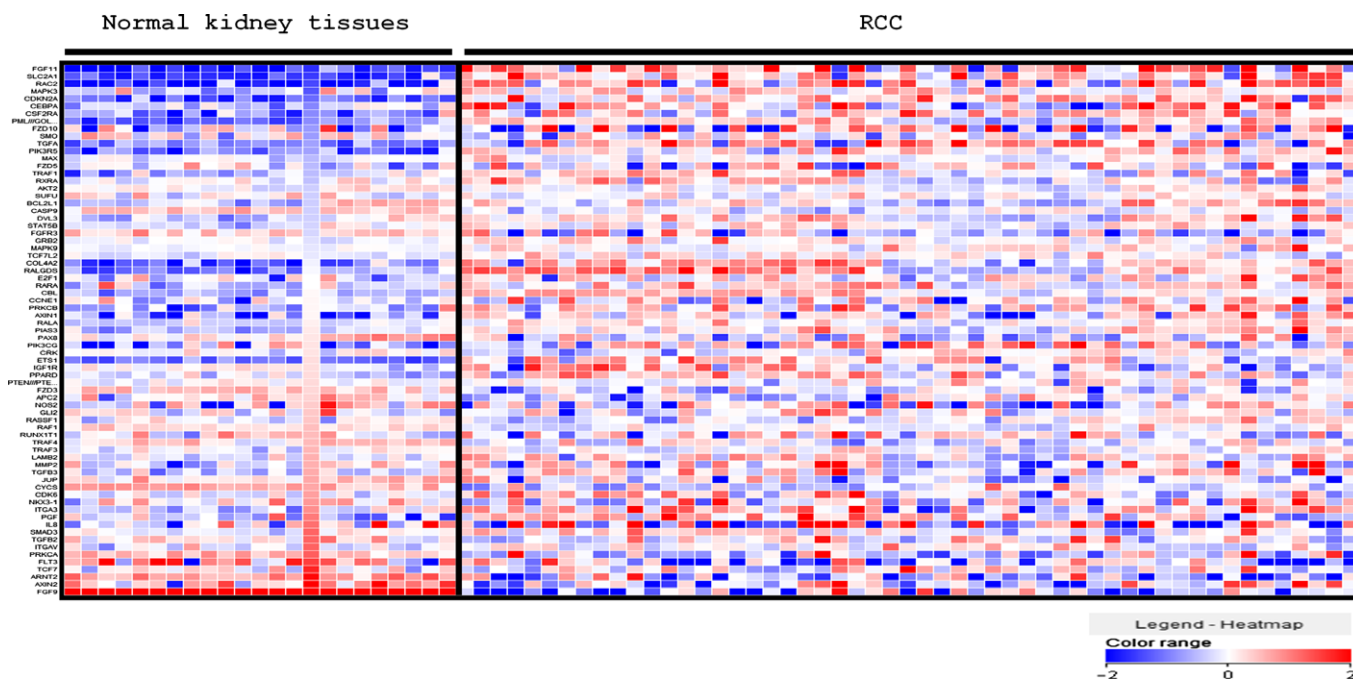


Fig. 3. Heat map diagram of the expression of 74 genes involved in 'pathways in cancer' in 53 renal cell carcinoma (RCC) specimens in comparison with 23 adjacent non-cancerous kidney specimens. Precise information of all 74 genes is summarized in Table S3.

find any positive correlation between *KANSL2* mRNA and *miR-1291* expression in the clinical samples and *KANSL2* mRNA expression was modest but *miR-1291* expression was quite faint in comparison with the internal control expression. These data suggest that they might have different mechanisms to regulate their expression even though *miR-1291* is nested in the *KANSL2* gene. Further examination is necessary to elucidate the silencing mechanisms of *miR-1291* expression. We did not find any correlation between *miR-1291* expression and clinico-pathological parameters. Our cohort included only five samples with pT3 and pT4 among 27 RCC and it was too small to evaluate the relationship between them.

Next, we investigated the functional significance of *miR-1291* in RCC by using two cell lines, A498 and 768-O. Furthermore, two types of miRNA (from Ambion and Thermo

were used to evaluate the function of *miR-1291*. Restoration of mature *miR-1291* in cancer cells showed significant inhibition of cancer cell proliferation, suggesting that *miR-1291* might indeed be a new tumor suppressor in RCC. A cell cycle assay revealed marked G0-G1 arrest in *miR-1291*-transfected A-498 cells but not in 786-O cells, suggesting that *miR-1291* might regulate genes associated with cell cycles in some RCC cases.

With the exception of our present report, no other studies have suggested relationships between tumor-suppressive *miR-1291* and human cancers. Thus, we believe that analysis of *miR-1291* could lead to discoveries of new molecular mechanisms in RCC. It is believed that a single miRNA is capable of targeting a number of genes to globally regulate biological processes. Aberrantly expressed miRNA causes disruption of the tightly regulated miRNA-messenger RNA networks in

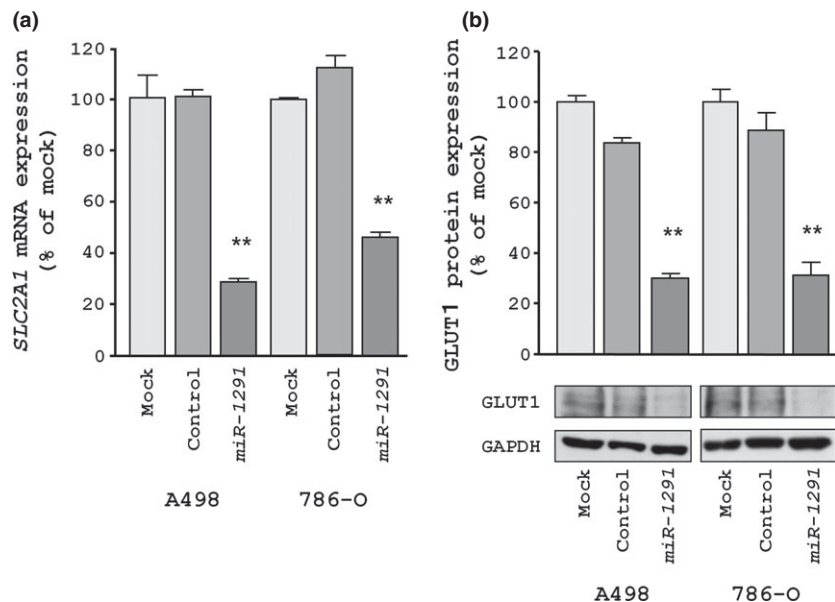


Fig. 4. *SLC2A1/GLUT1* as a target gene of *miR-1291* in renal cell carcinoma (RCC). (a) *SLC2A1/GLUT1* mRNA expression at 24 h after transfection with 10 nM *miR-1291*. (b) *SLC2A1/GLUT1* protein expression at 72 h after transfection with microRNA. GAPDH was used as a loading control. (c) *miR-1291* binding sites in the 3'UTR of *SLC2A1/GLUT1* mRNA. Luciferase reporter assays used the three types of vectors encoding the partial 3'UTR of *SLC2A1/GLUT1* mRNA. The first deletion vector was constructed as lacking position 607-613 of putative *miR-1291* target sites (del-1). The second deletion vector was constructed as lacking position 649-655 of putative *miR-1291* target sites (del-2). The third deletion vector was constructed as lacking both positions of *miR-1291* target sites (del-1 and del-2). *Renilla* luciferase values were normalized to corresponding firefly luciferase values. * $P < 0.05$; ** $P < 0.0001$.

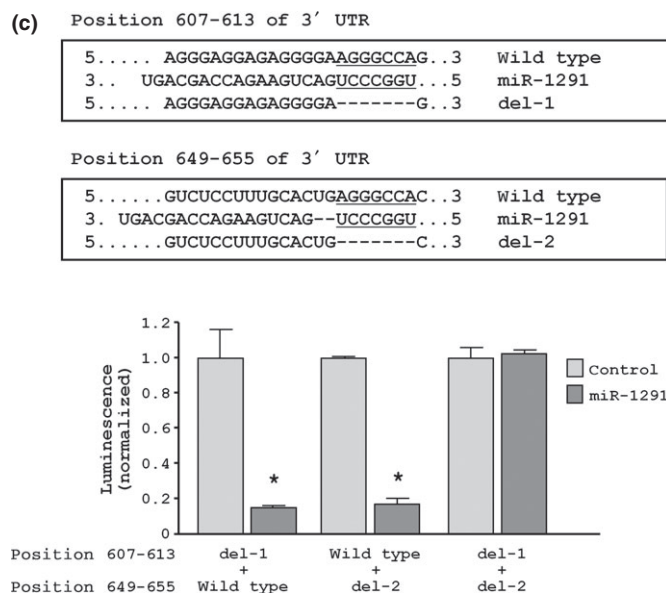


Fig. 5. *SLC2A1/GLUT1* mRNA and *miR-1291* expression in clinical specimens. (a) *SLC2A1/GLUT1* mRNA expression in 27 clinical renal cell carcinoma (RCC) specimens and 27 adjacent normal specimens. (b) An inverse correlation between *SLC2A1/GLUT1* mRNA and *miR-1291* expression in clinical specimens.

cancer cells. Therefore, we propose that identification of novel cancer pathways and target genes regulated by tumor-suppressive *miR-1291* is an important first step in understanding RCC

oncogenesis. To elucidate the tumor-suppressive functions of *miR-1291*, we investigated the molecular pathways and target oncogenic genes regulated by *miR-1291* in RCC cells. A total

of 3363 targets were categorized into known molecular pathways using KEGG pathways and the 'pathways in cancer' category was selected as the pathway that was most significantly regulated by *miR-1291*. Furthermore, we searched for driver genes in RCC involved in the 'pathways in cancer' category. In the present study, we selected *SLC2A1/GLUT1* because this gene was upregulated in RCC clinical specimens and reduced by *miR-1291* transfection in RCC cells. Luciferase reporter assays demonstrated that *miR-1291* directly targeted *SLC2A1/GLUT1*. This is the first report demonstrating that *SLC2A1/GLUT1* was regulated by a specific miRNA.

Glucose regulates transcription, enzymatic activity and hormone secretion. These functions typically depend on glucose uptake, which is primarily controlled by the glucose transporters family (*GLUT1-14*).^(21,22) There are 14 GLUT members, of which *GLUT1*, the first member of the GLUT family to be identified, is the most extensively studied. *GLUT1* was reported originally as a marker of infantile skin hemangioma⁽²³⁾ and overexpression was reported in several types of human cancers, including RCC.⁽²⁴⁻³¹⁾ Renal cell carcinomas, like many other cancers, are dependent on aerobic glycolysis for ATP production, a phenomenon known as the Warburg effect.⁽¹⁰⁻¹²⁾ The dependence of RCC on glycolysis is in part a result of induction of *GLUT1*. In normal tissues, the product of the *VHL* gene is associated with ubiquitination and degradation of hypoxia inducible factor (HIF) through an oxygen-sensing mechanism.^(32,33) In the absence of oxygen or in the presence of a mutated *VHL* gene, HIF1a and HIF2a are stabilized and induce the expression of a panel of transcriptional target

genes, such as *VEGF*, *PDGF* and *GLUT1*, supporting the metabolic shift that underlies RCC tumorigenicity.⁽³⁴⁾ Interestingly, it was reported about the identification of a class of compounds; one member of this class, STF-31, selectively kills RCC by specifically targeting glucose uptake through *GLUT1*. Treatment with these agents inhibits the growth of RCC by binding *GLUT1* directly and impeding glucose uptake *in vivo* without toxicity to normal tissues.⁽³⁵⁾ *GLUT1* is a promising target for cancer treatment and *GLUT1*-regulated miRNA could possibly be used in nucleic acid medicine.

In conclusion, we found that downregulation of *miR-1291* was a frequent event in RCC. *miR-1291* inhibited cancer cell proliferation through direct targeting of *SLC2A1/GLUT1*, suggesting that *miR-1291* is a new tumor-suppressive miRNA. Tumor-suppressive *miR-1291* appeared to modulate multiple cancer-associated pathways. The recognition of oncogenes targeted by *miR-1291* might lead to a better understanding of RCC oncogenesis and promote the development of new therapeutic strategies for RCC.

Acknowledgments

The authors thank Ms Mutsumi Miyazaki for her excellent laboratory assistance.

Disclosure Statement

The authors have no conflict of interest.

References

- Gupta K, Miller JD, Li JZ *et al*. Epidemiologic and socioeconomic burden of metastatic renal cell carcinoma (mRCC): a literature review. *Cancer Treat Rev* 2008; **34**: 193–205.
- Hadoux J, Vignot S, De La Motte Rouge T. Renal cell carcinoma: focus on safety and efficacy of temsirolimus. *Clin Med Insights Oncol* 2010; **4**: 143–54.
- Griffioen AW, Mans LA, de Graaf AM *et al*. Rapid angiogenesis onset after discontinuation of sunitinib treatment of renal cell carcinoma patients. *Clin Cancer Res* 2012; **18**: 3961–71.
- Mattick JS. RNA regulation: a new genetics? *Nat Rev Genet* 2004; **5**: 316–23.
- Filipowicz W, Bhattacharyya SN, Sonenberg N. Mechanisms of post-transcriptional regulation by microRNAs: are the answers in sight? *Nat Rev Genet* 2008; **9**: 102–14.
- Bartel DP. MicroRNAs: genomics, biogenesis, mechanism, and function. *Cell* 2004; **116**: 281–97.
- Nelson KM, Weiss GJ. MicroRNAs and cancer: past, present, and potential future. *Mol Cancer Ther* 2008; **7**: 3655–60.
- Esquela-Kerscher A, Slack FJ. Oncomirs – microRNAs with a role in cancer. *Nat Rev Cancer* 2006; **6**: 259–69.
- Hidaka H, Seki N, Yoshino H *et al*. Tumor suppressive microRNA-1285 regulates novel molecular targets: aberrant expression and functional significance in renal cell carcinoma. *Oncotarget* 2012; **3**: 44–57.
- Warburg O. On the origin of cancer cells. *Science* 1956; **123**: 309–14.
- Gogvadze V, Zhivotovsky B, Orrenius S. The Warburg effect and mitochondrial stability in cancer cells. *Mol Aspects Med* 2010; **31**: 60–74.
- Vander Heiden MG, Cantley LC, Thompson CB. Understanding the Warburg effect: the metabolic requirements of cell proliferation. *Science* 2009; **324**: 1029–33.
- Sommermann TG, O'Neill K, Plas DR *et al*. IKK β and NF- κ B transcription govern lymphoma cell survival through AKT-induced plasma membrane trafficking of *GLUT1*. *Cancer Res* 2011; **71**: 7291–300.
- Sobin LH, Wittekind C. *TNM Classification of Malignant Tumours*, 6th edn. International Union Against Cancer (UICC). New York: Wiley-Liss Inc., 2009; 255–257.
- Chiyomaru T, Enokida H, Tatarano S *et al*. miR-145 and miR-133a function as tumour suppressors and directly regulate *FSCN1* expression in bladder cancer. *Br J Cancer* 2010; **102**: 883–91.
- Nohata N, Hanazawa T, Kikkawa N *et al*. Caveolin-1 mediates tumor cell migration and invasion and its regulation by miR-133a in head and neck squamous cell carcinoma. *Int J Oncol* 2011; **38**: 209–17.

- Kawakami K, Enokida H, Chiyomaru T *et al*. The functional significance of miR-1 and miR-133a in renal cell carcinoma. *Eur J Cancer* 2012; **48**: 827–36.
- Davis-Dusenbery BN, Hata A. MicroRNA in cancer: the involvement of aberrant microRNA biogenesis regulatory pathways. *Genes Cancer* 2010; **1**: 1100–14.
- Yamasaki T, Seki N, Yamada Y *et al*. Tumor suppressive microRNA-138 contributes to cell migration and invasion through its targeting of vimentin in renal cell carcinoma. *Int J Oncol* 2012; **41**: 805–17.
- Yamada Y, Hidaka H, Seki N *et al*. Tumor-suppressive microRNA-135a inhibits cancer cell proliferation by targeting the *c-MYC* oncogene in renal cell carcinoma. *Cancer Sci* 2013; **104**: 304–12.
- Macheda ML, Rogers S, Best JD. Molecular and cellular regulation of glucose transporter (GLUT) proteins in cancer. *J Cell Physiol* 2005; **202**: 654–62.
- Joost HG, Thorens B. The extended GLUT-family of sugar/polyol transport facilitators: nomenclature, sequence characteristics, and potential function of its novel members (review). *Mol Membr Biol* 2001; **18**: 247–56.
- North PE, Waner M, Mizeracki A *et al*. *GLUT1*: a newly discovered immunohistochemical marker for juvenile hemangiomas. *Hum Pathol* 2000; **31**: 11–22.
- Ozcan A, Shen SS, Zhai QJ *et al*. Expression of *GLUT1* in primary renal tumors: morphologic and biologic implications. *Am J Clin Pathol* 2007; **128**: 245–54.
- Nagase Y, Takata K, Moriyama N *et al*. Immunohistochemical localization of glucose transporters in human renal cell carcinoma. *J Urol* 1995; **153**: 798–801.
- Jang SM, Han H, Jang KS *et al*. The glycolytic phenotype is correlated with aggressiveness and poor prognosis in invasive ductal carcinoma. *J Breast Cancer* 2012; **15**: 172–80.
- Brown RS, Wahl RL. Overexpression of *GLUT-1* glucose transporter in human breast cancer. An immunohistochemical study. *Cancer* 1993; **72**: 2979–85.
- Mellanen P, Minn H, Grenman R *et al*. Expression of glucose transporters in head-and-neck tumors. *Int J Cancer* 1994; **56**: 622–9.
- Kawamura T, Kusakabe T, Sugino T *et al*. Expression of glucose transporter-1 in human gastric carcinoma: association with tumor aggressiveness, metastasis and patient survival. *Cancer* 2001; **92**: 634–41.
- Rudlowski C, Becker AJ, Schroder W *et al*. *GLUT1* messenger RNA and protein induction relates to the malignant transformation of cervical cancer. *Am J Clin Pathol* 2003; **120**: 691–8.
- Cantuaria G, Fagotti A, Ferrandina G *et al*. *GLUT1* expression in ovarian carcinoma: association with survival and response to chemotherapy. *Cancer* 2001; **92**: 1144–50.

- 32 Jaakkola P, Mole DR, Tian YM *et al.* Targeting of HIF-alpha to the von Hippel-Lindau ubiquitylation complex by O2-regulated prolyl hydroxylation. *Science* 2001; **292**: 468–72.
- 33 Kaelin WG Jr. Molecular basis of the VHL hereditary cancer syndrome. *Nat Rev Cancer* 2002; **2**: 673–82.
- 34 Smaldone MC, Maranchie JK. Clinical implications of hypoxia inducible factor in renal cell carcinoma. *Urol Oncol* 2009; **27**: 238–45.
- 35 Chan DA, Sutphin PD, Nguyen P *et al.* Targeting GLUT1 and the Warburg effect in renal cell carcinoma by chemical synthetic lethality. *Sci Transl Med* 2011; **3**: 94ra70.

Supporting Information

Additional supporting information may be found in the online version of this article:

Fig. S1. Expression levels of *miR-1291* in 20 human cancer cell lines.

Fig. S2. Cell cycle assays in *miR-1291*-transfected renal cell carcinoma cell lines.

Fig. S3. Strategy for selection of *miR-1291* target genes.

Table S1. Significantly enriched annotations regulated by *miR-1291* in the TargetScan database.

Table S2. Candidate target genes of *miR-1291* involved in ‘pathways in cancer’.

Table S3. Seventy-four differently expressed genes involved in the ‘pathway in cancer’.